HAL
open science

Electrochemical analysis of a microbial electrochemical snorkel in laboratory and constructed wetlands

Joanna Rogińska, Michel Perdicakis, Cédric Midoux, Théodore Bouchez, Christelle Despas, Liang Liu, Jiang-Hao Tian, Cédric Chaumont, Frédéric P.A. Jorand, Julien Tournebize, et al.

To cite this version:

Joanna Rogińska, Michel Perdicakis, Cédric Midoux, Théodore Bouchez, Christelle Despas, et al.. Electrochemical analysis of a microbial electrochemical snorkel in laboratory and constructed wetlands. Bioelectrochemistry, 2021, 142, pp.107895. 10.1016/j.bioelechem.2021.107895 . hal-03318075

HAL Id: hal-03318075

https://hal.inrae.fr/hal-03318075v1

Submitted on 9 Aug 2021

HAL is a multi-disciplinary open access archive for the deposit and dissemination of scientific research documents, whether they are published or not. The documents may come from teaching and research institutions in France or abroad, or from public or private research centers.

L'archive ouverte pluridisciplinaire **HAL**, est destinée au dépôt et à la diffusion de documents scientifiques de niveau recherche, publiés ou non, émanant des établissements d'enseignement et de recherche français ou étrangers, des laboratoires publics ou privés.

Bioelectrochemistry 142 (2021) 107895

Contents lists available at ScienceDirect

Bioelectrochemistry

journal homepage: www.elsevier.com/locate/bioelechem

Electrochemical analysis of a microbial electrochemical snorkel in laboratory and constructed wetlands

Joanna Rogińska [a], Michel Perdicakis [a], Cédric Midoux [c], Théodore Bouchez [c], Christelle Despas [a], Liang Liu [a], Jiang-Hao Tian [c], Cédric Chaumont [b], Frédéric P. A. Jorand [a], Julien Tournebize [b], Mathieu Etienne [a,*]

[a] Université de Lorraine, CNRS, LCPME, F-54000 Nancy, France
[b] UR HYCAR, Université de Paris Saclay, INRAE, centre d'Antony, 92761, Antony Cedex, France
[c] UR PROSE, Université de Paris Saclay, INRAE, centre d'Antony, 92761 Antony Cedex, France

ARTICLE INFO

Article history:
Received 27 April 2021
Received in revised form 19 July 2021
Accepted 21 July 2021
Available online 24 July 2021

Keywords:
Microbial fuel cells
Microbial electrochemical snorkel
Denitrification
Biocathode
Bioanode

ABSTRACT

Microbial electrochemical snorkel (MES) is a short-circuited microbial fuel cell applicable to water treatment that does not produce energy but requires lower cost for its implementation. Few reports have already described its water treatment capabilities but no deeper electrochemical analysis were yet performed. We tested various materials (iron, stainless steel and porous graphite) and configurations of snorkel in order to better understand the rules that will control in a wetland the mixed potential of this self-powered system. We designed a model snorkel that was studied in laboratory and on the field. We confirmed the development of MES by identifying anodic and cathodic parts, by measuring the current between them and by analyzing microbial ecology in laboratory and field experiments. An important application is denitrification of surface water. Here we discuss the influence of nitrate on its electrochemical response and denitrification performances. Introducing nitrate caused the increase of the mixed potential of MES and of current at a potential value relatively more positive than for nitrate-reducing biocathodes described in the literature. The major criteria for promoting application of MES in artificial wetland dedicated to mitigation of non-point source nitrate pollution from agricultural water are considered.
© 2021 Elsevier B.V. All rights reserved.

1. Introduction

Microbial Fuel Cells (MFC) are bioelectrochemical systems widely studied for energy production and water treatment [1]. However, their application for water decontamination in the environment is still limited. A simpler possible solution is to use the Microbial Electrochemical Snorkel (MES) that is a short-circuited MFC in which the electrons produced in oxidation reaction on bioanode in sediment can freely flow towards the biocathode in water where they can be used in reduction (Scheme 1). The potential of the electrode is therefore a mixed potential [2] and no power can be produced in this configuration, but high current can be achieved. As a result, the water decontamination could be more efficient [3]. The concept was introduced in 2011 [4] when the group of Bergel studied both "short-circuited MFC" composed of graphite felt anode connected in short-circuit with Pt carbon-felt air-breathing cathode, and MES composed of colonized graphite felt as anode on the lower end of titanium rod and platinum on its top. They were used to remove the chemical oxygen demand from wastewater. The mixed potential of the two electrodes connected in short-circuit was +0.228 mV vs Standard Hydrogen Electrode (SHE). Other experiments proved that graphite rod snorkel can be used as direct electron acceptor for respiration and growth of *Shewanella decolorationis* [5]. Cruz-Viggi et al. mixed sediment contaminated with crude oil with granular activated carbon and placed a graphite rod which ensured an electrochemical connection between anoxic sediment and oxygenated overlying water [6]. The same group reported that insertion of simple graphite electrode snorkel half buried in the contaminated sediment and half exposed to water increases the sulfate reduction comparing to the snorkel-less control, causing in the same time accumulation of iron oxides on the surface of the electrode [7]. The other work made a great step towards the application of snorkel for water decontamination by using coke as electroconductive material to build the Electroactive Biofilm-Based Constructed Wetland which was efficiently removing organic matter, ammonium and phosphate. They also measured electric potential profiles on the depths of the sediment [8]. Recently, the first evidence of applicability of MES for metal recovery was described [9]. However, the electro-

* Corresponding author.
E-mail address: mathieu.etienne@univ-lorraine.fr (M. Etienne).

https://doi.org/10.1016/j.bioelechem.2021.107895
1567-5394/© 2021 Elsevier B.V. All rights reserved.

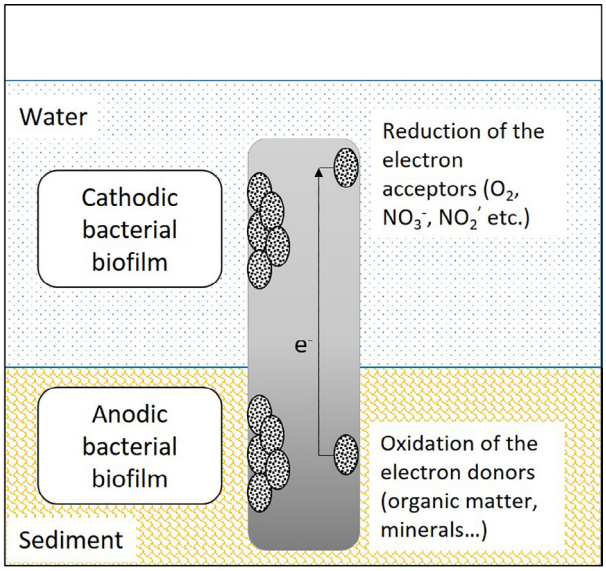

Scheme 1. Scheme of a Microbial Electrochemical Snorkel. The anodic bacterial biofilm oxidizes the electron donors present in the sediment. The electrons released in this process are collected by the Snorkel and transported to the part in water. Then, they can be used for the reduction of electron acceptors present in water by the cathodic bacterial biofilm.

chemical studies of the processes on sediment and water parts have not yet been described.

Fertilizer production in Haber-Bosh process or biological N_2 fixation caused by substantial legume crops result in perturbation of natural N cycle [10]. Consequently, the water draining from agricultural fields to water reservoirs such as lakes or rivers is often polluted and one of the main contaminations is nitrate leading to Nitrate Framework Directive (1990–2000). The high concentration of nitrate in water may cause several negative environmental effects such as eutrophication or increased emission of nitrous oxide (N_2O), a greenhouse gas which is an intermediate in reactions of nitrification and denitrification [11]. Denitrification is here a microbial process of nitrogen oxides reduction (nitrate NO_3^- or nitrite NO_2^-) to gaseous oxides (nitric oxide NO and nitrous oxide NO_2) which then can be reduced to dinitrogen N_2 [12]. One of the proposed solutions for such water issues for mitigating excess nitrate are constructed wetlands – engineered systems designed to use the natural processes such as vegetation, sediments and microbial communities of wetlands to assist in denitrifying wastewater [13]. However, this approach might be not fast enough, especially in periods when the nitrate concentration is very high and if the wetland is not sufficiently big. The nitrate removal requires availability of organic electron donors and anaerobic or anoxic conditions [13]. The main reservoir of electrons is likely located in the anoxic sediments while the nitrates are more concentrated in the bulk water. One solution is to implement a microbial electrochemical technology with nitrate-reducing biocathode which would accelerate or stimulate the nitrate removal with the use of electrons coming from the oxidation of the organic matter in the sediments.

According to the literature related to microbial fuel cells (MFC), nitrate reducing biocathode can be developed by poising the electrode with the proper potential, which should be low enough to drive bacterial metabolism while avoiding hydrogen evolution [14]. According to Clauwaert et al., when the potentials are higher than 0 mV vs. SHE, the reduction of nitrogen oxides is negatively affected and therefore no higher denitrification rates can be obtained on cathodes with high potential [15]. It is moreover reported that applying to an electrode a potential in the region from −100 to −300 mV vs. SHE should allow to grow the nitrate-reducing biocathode [14,16–20]. However, these experiments were performed under an inert gas to eliminate oxygen (O_2) that interferes with nitrate reduction. Zhang and Angelidaki observed the decrease of nitrate removal rate by MFC with increasing concentration of oxygen in water [21]. In order to reduce nitrate, it is thus necessary to remove the oxygen, for example by creating anoxic zones.

The number of studies about nitrate reduction in MES configuration is still limited, probably because there are several challenges which need to be solved beforehand, like competition between reduction of oxygen and nitrate, or reducing the costs of such operation. Although Wang et al. did not use directly the snorkel, they noticed a decrease of power and an increase of current and nitrate removal efficiency with decrease of the applied resistance between some graphite felt electrodes of a sediment MFC, which was acclimated in a lake and later studied in conditions imitating natural [22]. With the resistance of 1 Ω they observed a 60% decrease of nitrate in 100 h, with initial concentration of 2.5 mg N-NO_3^- L^{-1}. This removal corresponds to (on average) 0.36 mg N-NO_3^- L^{-1} day^{-1}. Denitrification of water by MES was also described by Yang et al. [23] who used snorkel composed of graphite felt and iron rod. In their study, with initial concentration of 2 mg N-NO_3^- L^{-1}, 98% of nitrate was removed in 16 days, which corresponds to 0.125 mg N-NO_3^- L^{-1} day^{-1}. Both of these publications have shown promising results, however, in both reports, the initial nitrate concentration was relatively low so it is not considered as "waters affected by pollution", e.g. by Nitrate Directive (91/676/EEC), which have more than 50 mg NO_3^- L^{-1} (i.e., 11.3 mg N-NO_3^- L^{-1}).

In this study we examined the electrode material (iron, stainless steel and porous graphite) and configuration in order to obtain the appropriate mixed potential for nitrate removal, without external polarization. We especially targetted the potential in the range from −300 to −100 mV vs. SHE which should be the most suitable for developing the nitrate-reducing biocathode. We designed a MES in which cathodic and anodic sides could be studied in their environments individually. The chosen configuration was prepared and installed in a laboratory and in a full size experimental constructed wetland and exposed to nitrate at a concentration relevant for such application. Electrochemistry and microbiology of both systems were then studied and compared, and the challenges of application of MES for denitrification are discussed.

2. Materials and methods

2.1. Materials

The sediments were collected from a constructed wetland of Rampillon (77, Seine-et-Marne, France [24,25]) and from a wetland in Ville sur Illon (88, Vosges, France [26]); both wetlands were built to intercept surface water and mitigate non-point source pollution from agricultural field (annual average nitrate concentration above 60 mg NO_3^- L^{-1}). All sediments were kept in a cool dark space (the composition of the sediments is provided in Supplementary material: Table S1 and S2). No significant differences in denitrification rates were observed between these two sediments so both were used; the origin of the sediment is indicated in the corresponding Table or Figure caption. Results obtained from Rampillon's sediment are presented in the manuscript and results obtained from Ville sur Illon's sediment are presented in Supplementary material. The synthetic water medium had following composition: 0.6 mM $CaSO_4$, 0.15 mM Na_2SO_4, 0.5 mM $NaHCO_3$, 0.2 mM NaCl, 0.2 mM KCl, 0.3 mM $MgCl_2$, which is based on the composition of the contracted wetland of Rampillon. In order to keep the natural condi-

tions, no additional buffers, vitamins or any other compounds were added to the reactor, except from addition of nitrate in order to follow denitrification. All experiments were performed in cylindrical reactors (d = 20 cm, height = 50 cm, S = 0.031 m^2) made of PMMA (Plexiglas), in which there was 5 cm of sediment and 25 cm of water unless otherwise stated. Graphite felt GFD6EA was provided by SGL, Germany. 316L stainless steel wire was provided by SAFFRO (∅ 1.2 mm). Stainless steel mesh 316L was provided by Gantois industries (St Die des Vosges, France) (∅ 0.56 mm, nominal aperture 1000 μm and 41% transparency). Iron bare (∅ 1 cm) and wire (∅ 1 mm) were taken from the laboratory stock. Stainless steel wires that we insulated with a heat-shrinking polymer tubing were used for all electrical connections with elements of the devices.

2.2. Preliminary experiments

In the initial experiment, eight different snorkels were compared for their potential application for biocathode in snorkel configuration. Four stainless steel wires and four iron wires were placed in two reactors, one for stainless steel and one for iron. All wires had the same length but different parts were exposed to water or sediment and isolated with plastic cover. The wire was accessible from outside of reactor for the potential measurement. Four configurations were tested with varying water:sediment ratios: 0:1; 1:1, 5:1, 1:0 (Table 1, Fig. S1). The potentials of the wires in these configuration were measured daily with a Methrom 605 pH-meter.

To choose the correct ratio between part in water and part in sediment, a similar experiment was tested but using stainless steel grid as electrodes in both sediment and water. Two ratios between water and sediment electrode were tested: they were either of the same size (8 × 4 cm) or the electrode in sediment was four times bigger than electrode in water (anode: two connected pieces 8 × 4 cm, one above another; cathode: 4 × 4 cm) (see Schematic S1 in Supplementary Material). All connections were done with isolated stainless steel wires.

Finally, in order to verify the influence of the material of electrode in water on the resulting mixed potential, graphite felt electrode in sediment (8 × 4 cm) and in water (3.5 × 1 cm) were connected with stainless steel wire (Fig. S3). A part of stainless steel wire was isolated from water and was accessible from outside of the reactor for monitoring of redox potentials. Two analogous experiments were also prepared with iron wire instead of stainless steel to confirm corrosion phenomena.

2.3. Model snorkel in laboratory wetland and in field constructed wetland

Eight pieces of stainless steel grid, of size 10 × 10 cm, were placed one above another in a distance of 0.5 cm (Scheme 2, electrodes #1–8). Two additional pieces, electrodes #9 and #10 were placed above them, so the electrode #9 was 1.5 cm above the electrode #8, and electrode #10 was 1 cm above #9. In order to keep this distance and avoid short cut between them, plastic separators were placed on the sides. Each electrode had a stainless steel wire attached, which was exposed to water only in the place of connection. These wires were connected above the level of water, so for most of the time the electrodes were connected all together in short-circuit and they were disconnected only for electrochemical measurements. A first system was placed in the plexiglas laboratory reactor. The same system was placed simultaneously in Rampillon on the 10.04.2019 in a small section of field water–sediment column delimited by a PVC tube of similar dimensions as the laboratory reactor, with openings that allowed the water to flow through. The acclimation lasted for over one month. The potential as well as concentration of nitrate were measured in the flowing water on the 10th of April, 20th of April and 15th of May 2019. Control experiments were also prepared in the laboratory, which consisted of stainless steel grid electrodes of the same size positioned either in the sediment or in water. Electrical connections were done as reported before.

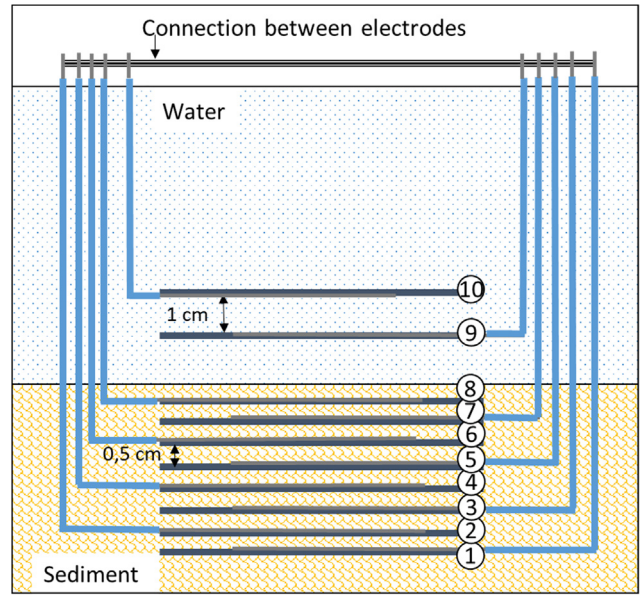

Scheme 2. Scheme of the Microbial Electrochemical Snorkel that was evaluated both in laboratory and *on-field*. The electrodes are numbered from the bottom (lowest Electrode #1, in sediment) to the top (highest Electrode #10, in water). The electrodes are made of stainless steel grid.

Table 1
Summary of redox potential studies of metallic wires connecting sediment and water in different ratios. The long-term potential after stabilization is given in the table; the day-by-day values are reported in Fig. S1 along with a scheme of the experiment. Sediments from Rampillon.

Material	Water:sediment ratio	E/mV (vs SHE)
Stainless steel	1:0 (only water)	Between +450 and +650
Stainless steel	0:1 (only sediment)	−250
Stainless steel	1:1 (sediment and water)	Between −140 and −150
Stainless steel	1:5 (sediment and water)	Between −140 and −150
Iron	1:0 (only water)	Below −400
Iron	0:1 (only sediment)	Below −400
Iron	1:1 (sediment and water)	Below −400
Iron	1:5 (sediment and water)	Below −400

2.4. Electrochemical studies

Electrochemical measurements were performed in the laboratory with potentiostat SP-150 Biologic in a two or in a three electrodes system. All potentials were measured versus SCE and reported hereafter versus SHE after proper correction ($E_{SCE/KClsat}$ = 0.248 V). The simultaneous potential and current measurement were obtained by connecting all electrodes in water as working electrode and all electrodes in sediment as counter electrode. Cyclic voltammetry (CV) was run at a scan rate of 1 mV s^{-1}. CV in the field were done with similar parameters, but with using a portable PalmSens4 potentiostat.

2.5. Ion chromatography

Ion chromatography was used to monitor the nitrate reduction rate. It was carried out using a Metrohm 882 Compact IC plus

instrument controlled by MagIC NetTM 3.1 software and equipped with chemical (Metrohm suppressor MSM II for chemical) and sequential (Metrohm CO_2 suppressor MCS) suppression modules and a conductivity detector. Separations were performed on a Metrosep A Supp 4-250/4.0 column packed with polyvinyl alcohol with quarternary ammonium groups (9 μm particle size) and associated with a guard column (Metrosep A supp 4/5 guard). The mobile phase consisted of a mixture of 1.8 mmol L^{-1} Na_2CO_3 and 1.7 mmol L^{-1} $NaHCO_3$ in ultrapure water (18.2 MV. cm at 293 K). The flow rate was 1 mL min^{-1} and the sample loop volume was 20 mL. Standard solutions were prepared from a commercial multi-element standard solution of 1000 mg mL^{-1} of NO_3^-, Cl^-, SO_4^{2-} and NO_2^- (SCP Science).

2.6. Microbial studies

The biofilm was detached from the electrode by placing the electrodes in sterile water and subjected to ultra-sonication (two treatments at 25 W for 1 min) from a probe positioned one centimeter above the coupon surface (VibraCell, 250 W, 20 kHz, probe of 10 mm in diameter, BioBlock Scientific).

The V4-V5 region of the 16S rRNA genes was amplified and sequence with the 515F (5′-GTGYCAGCMGCCGCGGTA-3′) and 928R (5′-CCCCGYCAATTCMTTTRAGT-3′) primers and the Ion Torrent PGM platform. All reads were imported into Galaxy to be proceeded with FROGS pipeline [27]. For the preprocessing, reads with length between 400 bp and 430 bp were kept. The clustering and chimera removal tools followed the guidelines of FROGS. OTUs with low abundance were trimmed by keeping only those appearing more than 0.005% in the whole dataset. Taxonomic assignment of OTUs was performed using Silva 132 SSU as reference database.

3. Results and discussion

3.1. Preliminary evaluation of materials

In the initial experiments, either stainless steel or iron were used to measure the redox potentials of these two electrode materials in different zones of a laboratory wetland. The goal was to evaluate if these potentials could be suitable to grow the nitrate-reducing biocathode, according to the data reported in the literature (i.e., in the range from −300 to −100 mV vs. SHE). For that, we used metallic wires placed in the reactor in the four different configurations shown on Fig. S1A. One wire was placed only in water (a) and another one only in sediment (b). Then, two samples were placed both in sediment and in water with different length ratios, i.e. with a longer section in sediment (c) and a similar length in sediment and in water (d). We examined first the behavior of stainless steel electrodes. When placed only in water (Table 1; Fig. S1B, curve a), the potential of the electrode reached values comprised between +450 and +650 mV vs SHE. Such potential values in natural (non-sterile) waters are often interpreted as dioxygen reduction potential of biocathode developed on stainless steel [28,29]. Note that no apparent corrosion was observed during the three months of this experiment.

When fully buried in the sediment (Table 1; Fig. S1B, curve b), the potential reached values of around −250 mV vs SHE. This is a typical value found as open circuit potential (OCP) of the bioanode in the literature [30]. Stainless steel wires which were then placed in the interface between sediment and water reached intermediate potential values that stabilize after about two months in a range that would be suitable for the growth of the desired biocathode, i.e. from −140 to −150 mV (Table 1; Fig. S1B, curves c&d).

Iron electrodes show a very different behavior. Regardless of the position, in water, in sediment or at the interface, all iron wires reached immediately very negative potential which was ranging from −400 to −500 mV vs SHE (Table 1). It was also observed soon after introducing the wires in the laboratory wetland that the wires became first orange before a thin layer of black residue deposited on the surface of sediment. Clearly, the potential values observed on iron are due to the corrosion of the metal in water and in sediment and not to oxidation of sediment electron donors that are expected at potentials higher than −300 mV vs SHE [31,32].

From this first series of experiments, we conclude that stainless steel electrodes positioned at the water sediment interface can reach the redox potential required to develop the biocathode without external polarization. Moreover, we suspect that iron would not be suitable because its potential was very negative, in relation with corrosion that was observed in the reactor.

In the next experiment we evaluated 316L stainless steel mesh basic material for the design of this microbial electrochemical snorkel (see Schematic S1 in Supplementary Material for illustration). Similarly as with wires, we implemented two different ratios between the surface of electrode buried in the sediment and the one positioned in water, i.e. 1:1 and 1:4 (four times bigger surface in sediment). In principle, the use of meshes allows to reach a much higher surface area to promote more efficiently electrochemical denitrification. Fig. 1A reports the evolution of potential with time. With ratio 1:4 (curve b), the potential reach rapidly −160 mV vs SHE, 65 mV more negative than with 1:1 ratio (curve a). Thus, we confirm here that stainless steel meshes can be used for the design of an electrochemical snorkel. A more negative mixed potential value is reached when higher surface is introduced in sediment than in water. As shown in Fig. 1B, when the contact between the two electrodes was open, the potential of both electrodes rapidly shifted within few hours from the mixed potential towards more negative values for the electrodes that are in sediment, and toward more positive values for the electrodes located in water. Therefore, the mixed potential reached by the snorkel is indeed a function of the individual electrode potentials and their relative surfaces.

Before going further, we have also performed few experiments with graphite felt that is widely used in electromicrobiology as electrode to support electroactive biofilms because of its very high surface area. An additional motivation was to evaluate experimentally a previous research reported few years ago that involved a microbial electrochemical snorkel composed of iron in water and graphite felt in the sediment [23]. Here, we first investigated the influence on the potential of the microbial electrochemical snorkel of graphite felt with either iron or stainless steel wires. The graphite felt was placed in sediment and connected with significantly smaller stainless steel or iron wires in water (see Schematic S2 in Supplementary Material for an illustration). The daily potential measurements for the experiment with stainless steel and graphite felt confirmed the expected role of graphite felt in sediment on the mixed potential of the whole system and the electrode reached a more negative potential (−240 mV vs SHE, Fig. 2, curve a) than with the stainless steel grid snorkel reported before (−160 mV vs SHE, Fig. 1A). Replacing the stainless steel wire with iron led to much lower potential (−467 mV vs SHE, Fig. 2, curve a'), a potential linked to the corrosion of iron metal that we discussed already. Although it was already described [23] the combination of graphite felt with iron appears not to be suitable for the construction of a microbial electrochemical snorkel, while the abiotic reactivity of metallic iron with nitrate should still be suitable for removal of nitrate [33,34]. Finally, based on this last experiment, we went further, by adding a piece of graphite felt on the metal wire located in water (See snorkel "b" in the scheme of Fig. S3). The motivation was to evaluate a microbial electrochemical snorkel composed only with highly porous graphite felt electrodes connected together with metal wires. The porous electrode in water was

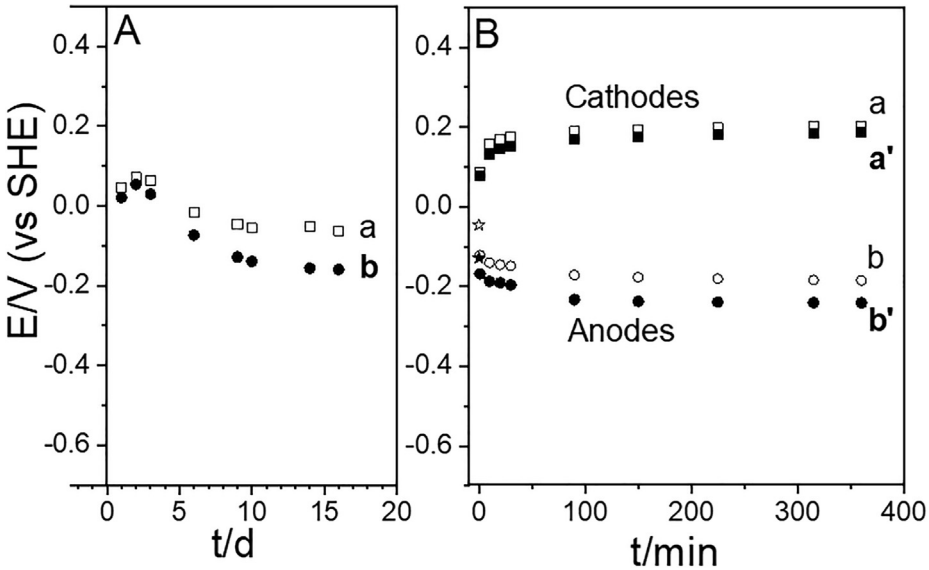

Fig. 1. Study of the influence of the electrode size in water and sediment on the potential of connected system. (A) Daily measurements of potentials of connected MES with different ratios: a - ratio 1:1; b - ratio 1:4. (B) Potential variation after disconnecting the two electrodes that are located one in sediment and the other in water. Points a (white squares) show the values for disconnected cathode for Ratio 1:1, a' (black squares) - for Ratio 1:4. Points b (white circles) show the values for disconnected anode for Ratio 1:1, b' (black circles) - for ratio 1:4. (Scheme of the experiment in Fig. S2 in Supplementary material).

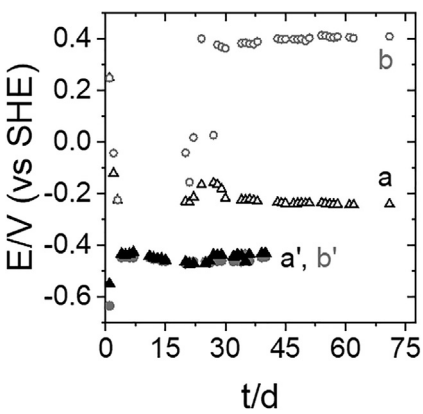

Fig. 2. Daily potential measurement with a MESs made of (a) graphite felt in sediment and metallic wire in water and (b) graphite felt in both sediment and water, connected together with a metallic wire. (a&b) were prepared with a stainless steel wire and (a'&b') with an iron wire. Sediments from Rampillon. Scheme of the experiment in Fig. S3 in Supplementary material.

much smaller than the one in sediment, with a ratio about 1:9. Despite this favorable design (large anode and small cathode), we observed that the potential of this graphite felt snorkel led to very high potential values, +400 mV vs SHE after two months in the laboratory wetland (Fig. 2, curve b). We did not observe so positive potentials when the stainless steel was tested, even when the ratio between anode and cathode was 1:1. This high value should not be suitable for nitrate reduction, and this design was not considered for next steps of this research. When stainless steel wire was replaced with iron, the situation was different but not more favorable. The potential of the snorkel was again very low, −450 mV vs SHE (Fig. 2, curve b'). In addition, a large amount of corrosion product was observed.

As a conclusion, a snorkel prepared with 316L stainless steel was found the most suitable to reach potentials below −100 mV vs SHE at the interface between sediment and water, without evidence of degradation of the system by corrosion. This material was used in the next step of this study as electrodes in both sediment and water in order to better study the influence on the electrochemical behavior of the environment surrounding the electrodes.

3.2. Design of the stainless steel snorkel and characterization

3.2.1. Experiments in a laboratory wetland

Scheme 2 reports the electrochemical snorkel that was designed and evaluated both in laboratory wetlands and *on-field* in the constructed wetland of Rampillon (France). The setup is composed of 10 stainless steel grid electrodes of 100 cm^2 each positioned parallel to each other from 0.5 cm in sediment and 1 cm in water. Numbering of the electrodes starts in the bottom (Electrode #1), up to the electrode positioned at the top (Electrode #10). All electrodes can be connected together at the top of the device and, once disconnected, can be analyzed individually.

Fig. 3A (points a) shows the redox potential of individual electrodes within this device, measured 4 days after the experiment started. From Electrode #1 to Electrode #8, all electrodes in the sediment have potential in the range between −120 and −280 mV vs SHE while Electrode #9 and Electrode #10 have a distinctive high potential of about +200 and +270 mV vs SHE. Because of this clear difference in the measured potentials, we made the hypothesis that all electrodes buried in the sediment would behave as anodes and the two electrodes in synthetic wastewater (Electrode #9 & Electrode #10) would behave as cathodes.

All anodes grouped together and all cathodes grouped together were connected to a potentiostat for measuring simultaneously their mixed potential and the current flowing between anodic and cathodic sides of this electrochemical snorkel (Fig. 3B). A relatively low current of −0.05 mA was observed at the beginning of the experiment and the potential value was close to 0. After about two days, the current reached a value in the range of −0.2 mA (curve I) and the potential of the snorkel decreased below −200 mV vs SHE (curve E). The values were kept in that range also after 6 days of starting the experiment, which proves that a snorkel was effectively created and the potential was in the range that is targeted in this study.

Cyclic voltammetric characterization was then performed on the different electrodes of this device, initially in the absence of

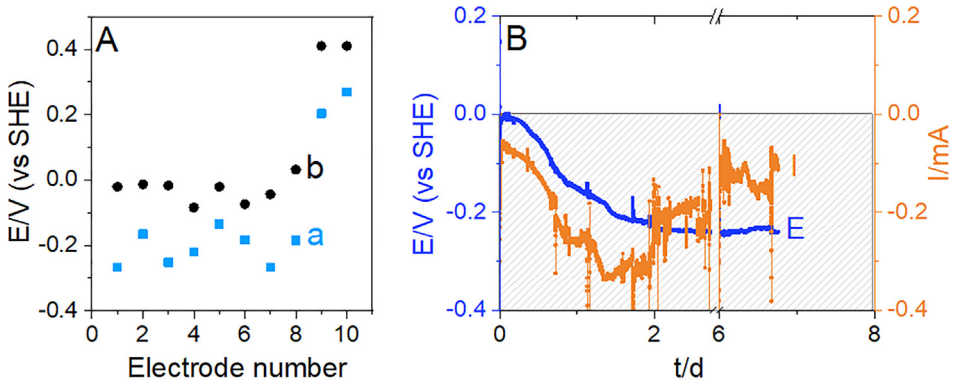

Fig. 3. (A) Open circuit potential of each electrode individually in absence of nitrate (a, blue squares) and presence of nitrate (b, black dotes). The potential was measured 1 h after disconnecting electrodes from the whole snorkel. (B) Mixed potential of all electrodes connected in short-circuit (blue line) and current flowing between Electrodes #1–#8 (anodes - in sediment) and Electrodes #9&#10 (cathodes – in water) (orange line). Sediments from Rampillon.

nitrate. Fig. 4A&B shows examples of voltammograms recorded with electrodes buried in sediment (A for Electrode #1 and B for Electrode #8). These curves are similar to each other, with voltammetric peak for both oxidation and reduction of the redox species present in the sediment. The more interesting signal should be located at the mixed potential of the snorkel and indeed, small oxidation peaks are found close to −100 mV. This oxidation current at anodes is responsible of the current flowing through the snorkel.

Electrode #9 and Electrode #10 that are considered as cathodic sides behave very differently (Fig. 4C&D). A very well defined cathodic wave is observed at +200 mV vs SHE that can be ascribed to the reduction of oxygen. This redox potential (+200 mV vs SHE) is in-between the typical potentials reported for oxygen biocathode [35]. The concentration of oxygen was ~4 mg L^{-1} (0.125 mmol L^{-1}), which was twice lower than in fresh tap water (~8 mg L^{-1}). The decease of oxygen concentration in the reactor compared to tap water could be associated with its consumption in the experiment.

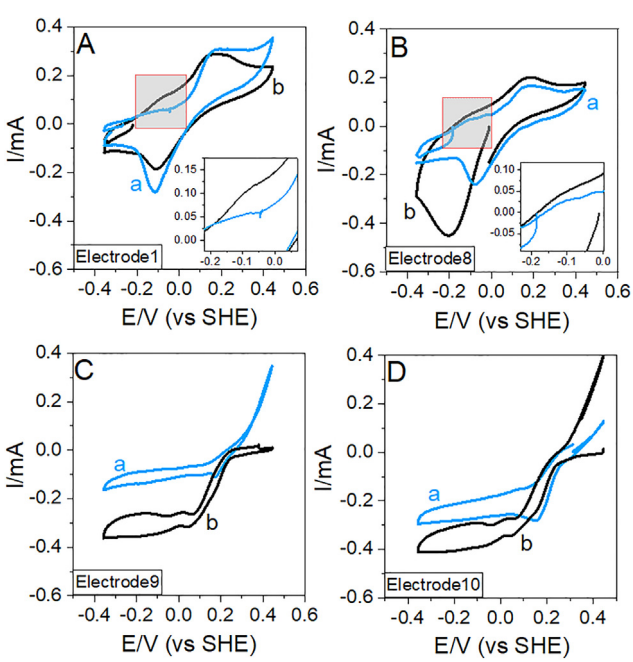

Fig. 4. Cyclic voltammetry of different electrodes in presence and absence of nitrate: (A) Electrode #1 (lowest position in sediment), (B) Electrode #8 (highest position in sediment), (C) Electrode #9 (lowest position in water) and (D) Electrode #10 (highest position in water). a (blue line) - without nitrate, b (black line) - with nitrate. Insets: zoom in the low potential region. Sediments from Rampillon.

At this moment, the bacterial diversity of the biofilms detached from the electrodes, sediment and water was analyzed with 16S rRNA gene analysis. All samples consisted of mixed communities of *Proteobacteria, Bacteroidetes, Cyanobacteria, Firmicutes, Planto-mycetes, Chloroflexi* and others, shown on Fig. 5. The bacteria in the sediment used for the inoculation was composed of major phyla: *Proteobacteria* 33%, *Bacteroidetes* 20%, *Firmicutes* 18%, *Cyanobacteria* 7%, *Acidobacteria* 6% and other *phyla* in less than 5% each. The biofilms on electrodes favored some *phyla* comparing to the community on sediment and water. Generally, on all electrodes the majority was *Proteobacteria* and *Bacteroidetes*, but the percentage of *Chloroflexi* was also more significant in biofilm electrodes than in sediment and water.

The dominating class of *Proteobacteria* was different for electrodes kept in sediment and those which were in water (see Table S3 in Supplementary Material). The microbial community on both lowest (#1) and highest (#8) electrodes in sediment showed that on stainless steel grid the main class was *δ-Proteobacteria*. *Geobacteriaceae* account for 33% of total community in Electrode #1 and 18% in Electrode #8 (see supplementary data). *Geobacteraceae* is a family which belongs to *δ -Proteobacteria* recognized for their ability to transfer electrons to electrodes and they are found on the anodes of microbial fuel cell [16]. Its ability to oxidize organic matter by coupling to solid electron acceptor, such as ferric oxides or anodes, was observed in several papers [36,37]. We conclude from the shape of CV and this 16S analysis that electrodes in sediment have clearly bioanodic behavior that was expected.

The community of electrodes in water was dominated by *γ-Proteobacteria* and *Bacteroidetes* (45.9 and 24.5% on Electrode #9 and 50.1 and 17% on Electrode #10, respectively). Debuy et al. also found that the oxygen-reducing stainless steel biocathode which they developed was also dominated by *γ-Proteobacteria* [38]. Similarly, Rothballer et al. obtained a monophyletic group of unclassified *γ-Proteobacteria* on their high-performing graphite plates biocathodes [39]. Sun et al. tested different biocathode carbon materials and found that *Bacteroidetes* and *Proteobacteria* were the dominant *phyla* on each of them [40]. It was also shown that O_2-reducing biocathodes dominated by mix of *Proteobacteria* and *Bacteroidetes* achieve significantly bigger current densities than biocathodes with pure culture [41]. It confirms the hypothesis that electrodes #9 and #10 behave like O_2-reducing biocathodes of dissolved oxygen in water column.

As a conclusion, we observed on each side of microbial electrochemical snorkel that there was specialized electroactive biofilms, which communities differed from the community in sediment or water.

The mean concentration of nitrate in the Rampillon's constructed wetland in spring is between 13 and 16 mg N-NO_3^- L^{-1}

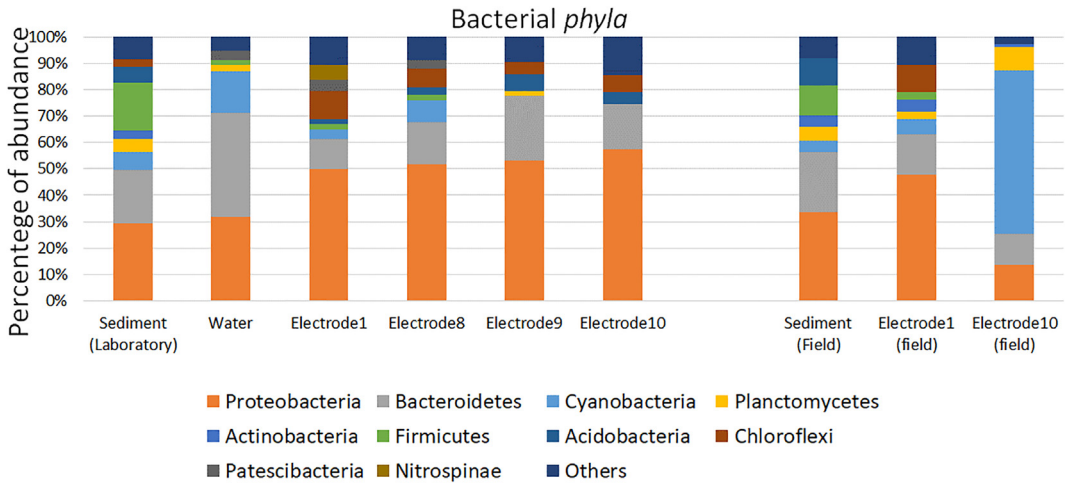

Fig. 5. Frequency distribution of bacterial community in sediment and water and on electrodes from 16S rRNA gene analysis.

but after fertilizer application it can reach around 40 mg N-NO_3^- L^{-1} [42] and therefore we decided to imitate this most extreme condition for which the device would be needed. After one month a large concentration of nitrate was thus introduced in solution (44 mg N-NO_3^- L^{-1}, 367 mg $NaNO_3$, 3.14 mmol NO_3^- L^{-1}).

The cyclic voltammetry performed 3 days after nitrate addition confirms that there was a big increase of cathodic current after nitrate addition (Fig. 4C&D). We observe a clear cathodic signal starting from at +250 mV followed by a cathodic wave starting around +50 mV on both Electrode #9 (Fig. 4C) and Electrode #10 (Fig. 4D). Cheng et al. built a photoelectrotrophic denitrification system in which they observed a nitrate reduction peak with half-wave potential close to 50 mV vs SHE [43]. Gregoire et al. observed similar shapes of the CVs of nitrate-reducing biocathode grown at potential of −250 mV vs Ag/AgCl (−55 mV vs SHE), leading in the presence of nitrate to a cathodic signal with half-wave potential at −200 mV vs Ag/AgCl (~0 mV vs SHE) [44]. Pous et al. found a nitrate reduction wave at −300 mV vs Ag/AgCl (~−100 mV vs SHE) [45] or around −150 mV vs SHE [18]. Yue et al. for the nitrate-reducing biocathode identified the wave beginning around −300 mV vs Ag/AgCl [46]. Therefore, the cathodic wave we observed in this manuscript in the presence of nitrate, in the region around 100 mV vs SHE is relatively more positive than in most of other studies. Moreover, it also cannot be associated with typical values for oxygen reduction, either more positive (~400 mV vs SHE) or closer to 0 V vs SHE [35].

Meanwhile, we observed some significant change in some CV responses recorded with the electrodes in sediment (Fig. 4B). After addition of nitrate, a very large reduction signal was observed with a peak at −200 mV vs SHE for Electrode #8. Moreover, we measured the OCP of every electrode individually again and we saw that the OCP of all anodes increased to reach a value close to 0 mV vs SHE; the OCP of cathodes increased also to the value around 400 mV (Fig. 3A). The mixed potential of the whole snorkel also shifted from negative values to +0.09 V and current increased to −0.55 mA.

Nitrate concentration was monitored simultaneously and compared with the control experiment which consisted of the same amount of the same sediment but without electrodes (See Fig. S2 in Supplementary Material). The experimental data was fitted to a simple model considering an apparent first order kinetic with $C = C_0e^{-kt}$. Based on the values from day 0 to 8, we observed the reaction constant k_{MES} = 0.03 ± 0.002 day^{-1} which is 25% higher than $k_{Control}$ = 0.022 ± 0.002 day^{-1}. The experiment was replicated with the sediment from Ville-sur-Illon and a similar behavior was observed (See Figs. S3 to S6 in Supplementary Material).

The most intriguing result comes from the relatively high potential observed in the presence of nitrate and the large cathodic signal that could be observed on some anodes (curve b in Fig. 4B; Figs. S4A&B and S5A&B in Supplementary Material) and we first considered that this change could come from nitrate that diffused into the sediment, interfering with bioanodic processes. It was shown in several papers that dioxygen diffuses into sediment only on very limited depth of about 2–3 mm [47,48], however nitrate diffusion and reduction in sediment is possible and was observed even on 20 cm of sediment depth [49,50]. A control experiment allowed to discard this hypothesis. Two individual electrodes of the same size were placed in the sediment and in water. As expected, these electrodes developed stable potentials after around 7 days from starting which was in the range of OCP of disconnected snorkel electrodes (225 mV vs SHE for the electrode in water and −250 mV vs SHE for the electrode in sediment). However, addition of nitrate to this control experiment did not change the OCP and the CV responses of these two individual electrodes (Fig. S7 in Supplementary Material).

Another explanation comes from the increase of current monitored at the cathodic side of the snorkel. Fig. 6 reports schematically two situations of the snorkel based on recorded electrochemical responses, depending on the activity of the biocathodic side, delivering low cathodic current (plain line) or high

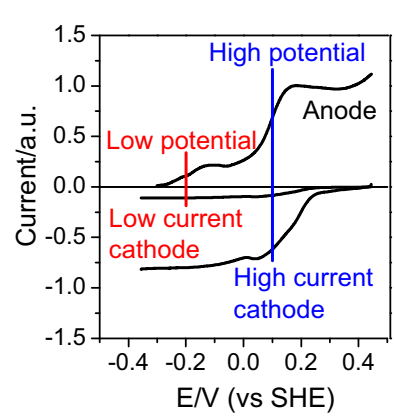

Fig. 6. Illustrative scenario leading to either low or high potential microbial electrochemical snorkel.

cathodic current (dashed line). The anodic side is considered more stable with time and only one typical current profile with potential is shown (current unit is here arbitrary). For small cathodic current, the potential of the electrochemical snorkel reaches the low potential region (−200 mV vs SHE for this scenario), with electron coming from a first anodic wave initiated around −300 mV vs SHE (see the insets in Fig. 4A&B). When higher current has to be delivered to the cathode, because of the higher activity of the electroactive biofilm or the higher concentration of oxygen over a sunny day, the high current potential has to be reached (+135 mV vs SHE for this second scenario).

The activity at higher potential could be associated to the accumulation at the surface of the anode of redox species that were detected electrochemically by cyclic voltammetry (for example, see curve b of Fig. 4B). The presence of nitrate in water and in sediment seems to promote the biocathodic activity of the microbial electrochemical snorkel, leading to a rapid transition from a low current biocathode to a high current biocathode. The higher activity of the biocathode requires then the higher current delivered by anode, so the anodic potential also must increase.

3.2.2. Acclimation in the constructed wetland of Rampillon (France)

The next step of this study was the introduction of the electrochemical snorkel in the constructed wetland of Rampillon (Seine-et-Marne, France), to evaluate further the phenomenon observed in the laboratory. A PVC tube, inserted in sediment-water column, allowed to define in the field a volume similar to the laboratory wetland. The snorkel was introduced in the wetland in spring. The natural conditions are very challenging, more light and more oxygen are present in the wetland. Moreover, less controlled composition of water and variations of the temperature are expected. During the period of evaluation, the potential of all connected electrodes was measured and water samples were taken to check the level of nitrate. On the 1st day, not more than one hour after the introduction, the potential value was +48 mV vs SHE and the concentration of nitrate was 30 mg NO_3^- L^{-1}. After 10 days those values were −189 mV and 10.8 mg NO_3^- L^{-1}. After 31st day the potential was +398 mV and nitrate concentration was 85.6 mg NO_3^- L^{-1}. These data confirm that nitrate concentration is influencing the mixed potential value of a snorkel that is more positive when a higher amount of nitrate is in water. Clauwaert *et al.* have seen such correlation and assumed that the potential of the cathode increases with higher current production, which is caused by higher nitrate loading rate [15]. However, it is also very likely that this high potential is caused by the increased concentration of oxygen. The day 31 of the experiment was very sunny therefore the oxygen amount in water was increased due to the activity of algae and cyanobacteria.

On the 31th day of the acclimation, the OCPs of all electrodes as well as CVs of Electrode #1 and Electrode #10 were performed in situ, in the wetland (Fig. 7A). As in the experiment in the laboratory, there is a difference in OCP of electrodes in contact with water and with sediment. The electrodes in sediment have the OCP in the same range as we showed before in the presence of nitrate. However, the electrodes in water had higher OCP values than it was in the laboratory, which were +500 mV vs SHE. This is the potential of biocathodic oxygen reduction [35]. The CV response recorded with Electrode #10 located in water (Fig. 7C) is different from the response in laboratory, however a small cathodic wave is observed, starting from potential around +500 mV vs. SHE, about 200 mV more positive than in the laboratory wetland. The CV of Electrode #1 located in the sediment has a very similar shape to CVs observed before in the laboratory in presence of nitrate (Fig. 7B).

Bacteria diversity analysis was performed also for two electrodes and sediment from the field (see Fig. 5). It shows again that the bacterial community is more diverse in the sediment than in the biofilm on electrodes, which consists mostly of bacteria from phyla *Proteobacteria* and *Bacteroidetes*. The microbial community is very similar in the sediment from the field and taken directly from the experiment started in the laboratory.

The community on anodic Electrode #1 (field) contains 37% of *δ-Proteobacteria*; 24% of whole community is from *Geobacteraceae* family (see supplementary data). Taking into consideration the shape of the CV and the community, we can say that it is very similar to the electrodes grown in the laboratory and therefore confirm that anodic biofilms were selected during *on-field* operation of the microbial electrochemical snorkel.

However, the specific conditions of the field influenced the biofilm on cathodic Electrode10 (field) which was very different from the Electrode #10 grown from the beginning in the laboratory. The community was dominated by *Cyanobacteria,* oxygenic phototroph bacteria (*algae*), favored because of the presence of light and oxygen during spring period. The consequence was a more effective oxygen biocathode and a mixed potential with high value, not a priori suitable for nitrate reduction.

4. Conclusion

The potential of the snorkel system depends on its material and on the proportion between electrode in water and in sediment. The best material for electrodes is stainless steel due to its proper mechanical and electrochemical properties, which allows reaching the proper potential. Using a four times bigger electrode in sediment than in water allows in laboratory to compensate the impact of oxygen reduction reaction and to achieve the potential value in

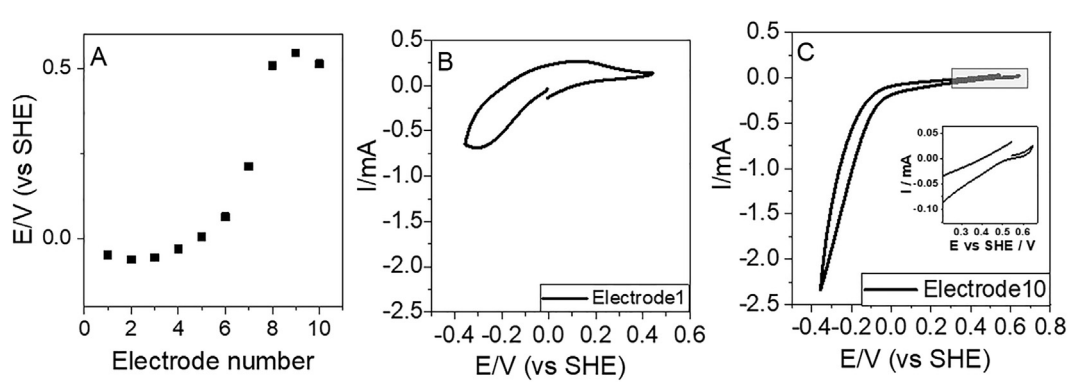

Fig. 7. Experiments performed in the wetland: (A) OCP of all electrodes, (B) Cyclic voltammetry of Electrode #1 and (C) Cyclic voltammetry of Electrode #10 (the gray area is enlarged).

range which is often used in the literature for developing nitrate reducing biocathode without applying it externally. This system allowed to develop a bioanode in a sediment and biocathode in water, between which there was a stable current flow. The shapes of CVs as well as microbial community studies confirm the anodic and cathodic roles of electrodes in sediment and water respectively. Addition of nitrate disturbed these conditions and led to an increase of the mixed potential of the system, which was caused by the increasing biocathodic activity linked to a 20–25% increase in the rate of nitrate removal. We observed a significant increase in current CV which could be linked with electrochemical nitrate reduction, at +100 mV vs SHE, which is relatively more positive value than for nitrate-reducing biocathodes described in the literature. The mixed potential of the device reached especially high value in the field, where the presence of sun induces growth of *Cyanobacteria* which increase the oxygen concentration. To operate biocathode for nitrate reduction in such sunny environment oversaturated with oxygen will impose to further optimize the architecture of the microbial electrochemical snorkel, to limit the interference from *Cyanobacteria* and other oxygenic photosynthetic planktons and by providing a ratio between anode and cathode to induce a mixed potential suitable for promoting nitrate reduction and denitrification *on-field*.

Declaration of Competing Interest

The authors declare that they have no known competing financial interests or personal relationships that could have appeared to influence the work reported in this paper.

Acknowledgments

Financial support from The French National Research Agency (ANR-17-CE04-0004) is gratefully acknowledged. We are grateful to the INRAE MIGALE bioinformatics facility (MIGALE, INRAE, 2020. Migale bioinformatics Facility, doi: 10.15454/1.5572390655343293E12) for providing computational resources. The authors would like to thank Timothé Philippon and Daryna Panicheva for the help with data treatment and Chrystelle Bureau for her contribution to the molecular biology and sequencing experiments. Bernard Saunier and his family are acknowledged for giving us access to the wetland of Ville sur Illon (France).

Appendix A. Supplementary data

Supplementary data to this article can be found online at https://doi.org/10.1016/j.bioelechem.2021.107895.

Chemical analysis of sediment composition, additional schemes, additional electrochemical results and nitrate removal results are included to support the discussion.

The detailed results of bacterial diversity analysis can be accessed by this address (biom file): https://doi.org/10.15454/KC3WAO

References

[1] B. Virdis, S. Freguia, R.A. Rozendal, K. Rabaey, Z. Yuan, J. Keller, Microbial fuel cells, Treatise Water Sci. 4 (2011) 641–665, https://doi.org/10.1016/B978-0-444-53199-5.00098-1.
[2] A.D. McNaught, A. Wilkinson, Compendium of Chemical Terminology, second ed. (the "Gold Book")., IUPAC, 2014.
[3] M. Hoareau, B. Erable, A. Bergel, Microbial electrochemical snorkels (MESs): A budding technology for multiple applications. A mini review, Electrochem. Commun. 104 (2019) 106473, https://doi.org/10.1016/j.elecom.2019.05.022.
[4] B. Erable, L. Etcheverry, A. Bergel, From microbial fuel cell (MFC) to microbial electrochemical snorkel (MES): maximizing chemical oxygen demand (COD) removal from wastewater, Biofouling 27 (2011) 319–326, https://doi.org/10.1080/08927014.2011.564615.
[5] Y. Yang, J. Guo, G. Sun, M. Xu, Characterizing the snorkeling respiration and growth of Shewanella decolorationis S12, Bioresour. Technol. 128 (2013) 472–478, https://doi.org/10.1016/j.biortech.2012.10.103.
[6] C. Cruz Viggi, E. Presta, M. Bellagamba, S. Kaciulis, S.K. Balijepalli, G. Zanaroli, M. Petrangeli Papini, S. Rossetti, F. Aulenta, The "Oil-Spill Snorkel": an innovative bioelectrochemical approach to accelerate hydrocarbons biodegradation in marine sediments, Front. Microbiol. 6 (2015) 881, https://doi.org/10.3389/fmicb.2015.00881.
[7] C. Cruz, B. Matturro, E. Frascadore, S. Insogna, A. Mezzi, S. Kaciulis, A. Sherry, O.K. Mejeha, I.M. Head, E. Vaiopoulou, K. Rabaey, S. Rossetti, F. Aulenta, Bridging spatially segregated redox zones with a microbial electrochemical snorkel triggers biogeochemical cycles in oil-contaminated River Tyne (UK) sediments, Water Res. 127 (2017) 11–21, https://doi.org/10.1016/j.watres.2017.10.002.
[8] C.A. Ramírez-Vargas, C.A. Arias, P. Carvalho, L. Zhang, A. Esteve-Núñez, H. Brix, Electroactive biofilm-based constructed wetland (EABB-CW): A mesocosm-scale test of an innovative setup for wastewater treatment, Sci. Total Environ. 659 (2019) 796–806, https://doi.org/10.1016/j.scitotenv.2018.12.432.
[9] M. Mitov, I. Bardarov, E. Chorbadzhiyska, K.L. Kostov, Y. Hubenova, First evidence for applicability of the microbial electrochemical snorkel for metal recovery, Electrochem. Commun. 122 (2021) 106889, https://doi.org/10.1016/j.elecom.2020.106889.
[10] S. Seitzngern, J.A. Harrison, J.K. Böhkle, A.F. Bouwman, R. Lowrance, B. Peterson, C. Tobias, G. Van Drecht, Denitrification across landscapes and waterscapes: A synthesis, Ecol. Appl. 16 (2006) 2064–2090, https://doi.org/10.1890/1051-0761(2006)016[2064:DALAWA]2.0.CO;2.
[11] D.E. Canfield, A.N. Glazer, P.G. Falkowski, The evolution and future of earth's nitrogen cycle, Science 330 (2010) 192–196, https://doi.org/10.1126/science.1186120.
[12] R. Knowles, Denitrification, Microbiol. Rev. 46 (1982) 43–70, https://doi.org/10.1128/mr.46.1.43-70.1982.
[13] J. Vymazal, Removal of nutrients in various types of constructed wetlands, Sci. Total Environ. 380 (2007) 48–65, https://doi.org/10.1016/j.scitotenv.2006.09.014.
[14] R. Tang, D. Wu, W. Chen, C. Feng, C. Wei, Biocathode denitrification of coke wastewater effluent from an industrial aeration tank : Effect of long-term adaptation, Biochem. Eng. J. 125 (2017) 151–160, https://doi.org/10.1016/j.bej.2017.05.022.
[15] P. Clauwaert, K. Rabaey, P. Aelterman, L. De Schamphelaire, T.H. Pham, P. Boeckx, N. Boon, W. Verstraete, Biological denitrification in microbial fuel cells, Environ. Sci. Technol. 41 (2007) 3354–3360, https://doi.org/10.1021/es062580r10.1021/es062580r.s001.
[16] K.B. Gregory, D.R. Bond, D.R. Lovley, Graphite electrodes as electron donors for anaerobic respiration, Environ. Microbiol. 6 (2004) 596–604, https://doi.org/10.1111/j.1462-2920.2004.00593.x.
[17] D. Molognoni, M. Devecseri, D. Cecconet, A.G. Capodaglio, Cathodic groundwater denitrification with a bioelectrochemical system, J. Water Process Eng. 19 (2017) 67–73, https://doi.org/10.1016/j.jwpe.2017.07.013.
[18] N. Pous, A.A. Carmona-Martínez, A. Vilajeliu-Pons, E. Fiset, L. Bañeras, E. Trably, M.D. Balaguer, J. Colprim, N. Bernet, S. Puig, Bidirectional microbial electron transfer: Switching an acetate oxidizing biofilm to nitrate reducing conditions, Biosens. Bioelectron. 75 (2016) 352–358, https://doi.org/10.1016/j.bios.2015.08.035.
[19] N. Pous, S. Puig, M. Dolors Balaguer, J. Colprim, Cathode potential and anode electron donor evaluation for a suitable treatment of nitrate-contaminated groundwater in bioelectrochemical systems, Chem. Eng. J. 263 (2015) 151–159, https://doi.org/10.1016/j.cej.2014.11.002.
[20] B. Virdis, K. Rabaey, Z. Yuan, R.A. Rozendal, J. Keller, Electron fluxes in a microbial fuel cells performing carbon and nitrogen removal, Environ. Sci. Technol. 43 (2009) 5144–5149, https://doi.org/10.1021/es8036302.
[21] Y. Zhang, I. Angelidaki, Bioelectrode-based approach for enhancing nitrate and nitrite removal and electricity generation from eutrophic lakes, Water Res. 46 (2012) 6445–6453, https://doi.org/10.1016/j.watres.2012.09.022.
[22] Y. Wang, J. Hu, L. Wang, D. Shan, X. Wang, Y. Zhang, X. Mao, L. Xing, D. Wang, Acclimated sediment microbial fuel cells from a eutrophic lake for the in situ denitrification process, RSC Adv. 6 (2016) 80079–80085, https://doi.org/10.1039/C6RA16510A.
[23] Q. Yang, H. Zhao, H.H. Liang, Denitrification of overlying water by microbial electrochemical snorkel, Bioresour. Technol. 197 (2015) 512–514, https://doi.org/10.1016/j.biortech.2015.08.127.
[24] J. Tournebize, C. Gramaglia, F. Birmant, S. Bouarfa, C. Chaumont, B. Vincent, Co-design of constructed wetlands to mitigate pesticide pollution in a drained catch-Basin: A solution to improve groundwater quality, Irrig. Drain. 61 (2012) 75–86, https://doi.org/10.1002/ird.1655.
[25] J.D. Lebrun, S. Ayrault, A. Drouet, L. Bordier, L.C. Fechner, E. Uher, C. Chaumont, J. Tournebize, Ecodynamics and bioavailability of metal contaminants in a constructed wetland within an agricultural drained catchment, Ecol. Eng. 136 (2019) 108–117, https://doi.org/10.1016/j.ecoleng.2019.06.012.
[26] C. Gaullier, S. Dousset, N. Baran, G. Kitzinger, C. Coureau, Influence of hydrodynamics on the water pathway and spatial distribution of pesticide and metabolite concentrations in constructed wetlands, J. Environ. Manage. 270 (2020) 110690, https://doi.org/10.1016/j.jenvman.2020.110690.
[27] F. Escudié, L. Auer, M. Bernard, M. Mariadassou, L. Cauquil, K. Vidal, S. Maman, G. Hernandez-Raquet, S. Combes, G. Pascal, FROGS: Find, Rapidly, OTUs with Galaxy Solution, Bioinformatics 34 (2018) 1287–1294, https://doi.org/10.1093/bioinformatics/btx791.

[28] V. Scotto, R. Di Cintio, G. Marcenaro, The infuence of marine aerobic microbial film on stainless steel corrosion behaviour, Corros. Sci. 25 (1985) 185–194, https://doi.org/10.1016/0010-938X(85)90094-0.
[29] D. Thierry, N. Larché, C. Leballeur, S.L. Wijesinghe, T. Zixi, Corrosion potential and cathodic reduction efficiency of stainless steel in natural seawater, Mater. Corros. 66 (2015) 453–458, https://doi.org/10.1002/maco.v66.510.1002/maco.201307497.
[30] L. Soussan, B. Erable, M. Delia, A. Bergel, The open circuit potential of Geobacter sulfurreducens bioanodes depends on the electrochemical adaptation of the strain, Electrochem. Commun. 33 (2013) 35–38, https://doi.org/10.1016/j.elecom.2013.04.013.
[31] B.E. Logan, J.M. Regan, Electricity-producing bacterial communities in microbial fuel cells, Trends Microbiol. 14 (2006) 512–518, https://doi.org/10.1016/j.tim.2006.10.003.
[32] D.A. Finkelstein, L.M. Tender, J.G. Zeikus, Effect of electrode potential on electrode-reducing microbiota, Environ. Sci. Technol. 40 (2006) 6990–6995, https://doi.org/10.1021/es061146m.
[33] C.-P. Huang, H.-W. Wang, P.-C. Chiu, Nitrate reduction by metallic iron, Water Res. 32 (1998) 2257–2264, https://doi.org/10.1016/S0043-1354(97)00464-8.
[34] J. Chi, S.-T Zhang, X. Lu, L.-H. Dong, S.-L. Yao, Chemical reduction of nitrate by metallic iron, J. Water Supply Res. Technol. 53 (2004) 37–41, https://doi.org/10.2166/aqua.2004.0004.
[35] M. Rimboud, A. Bergel, B. Erable, Multiple electron transfer systems in oxygen reducing biocathodes revealed by different conditions of aeration/agitation, Bioelectrochemistry 110 (2016) 46–51, https://doi.org/10.1016/j.bioelechem.2016.03.002.
[36] D.R. Bond, D.R. Lovley, Electricity Production by Geobacter sulfurreducens Attached to Electrodes, Appl. Environ. Microbiol. 69 (2003) 1548–1555, https://doi.org/10.1128/AEM.69.3.1548.
[37] D.R. Bond, D.E. Holmes, L.M. Tender, D.R. Lovley, Electrode-reducing microorganisms that harvest energy from marine sediments, Science 295 (2002) 483–485, https://doi.org/10.1126/science.1066771.
[38] S. Debuy, S. Pecastaings, A. Bergel, B. Erable, Oxygen-reducing biocathodes designed with pure cultures ofmicrobial strains isolated from seawater biofilms, Int. Biodeterior. Biodegrad. 103 (2015) 16–22, https://doi.org/10.1016/j.ibiod.2015.03.028.
[39] M. Rothballer, M. Picot, T. Sieper, J.B.A. Arends, M. Schmid, A. Hartmann, N. Boon, C.J.N. Buisman, F. Barrière, D.P.B.T.B. Strik, Monophyletic group of unclassified γ-Proteobacteria dominates in mixed culture biofilm of high-performing oxygen reducing biocathode, Bioelectrochemistry 106 (2015) 167–176, https://doi.org/10.1016/j.bioelechem.2015.04.004.
[40] Y. Sun, J. Wei, P. Liang, X. Huang, Microbial community analysis in biocathode microbial fuel cells packed with different materials, AMB Express. 2 (2012) 21, https://doi.org/10.1186/2191-0855-2-21.
[41] K. Rabaey, S.T. Read, P. Clauwaert, S. Freguia, P.L. Bond, L.L. Blackall, J. Keller, Cathodic oxygen reduction catalyzed by bacteria in microbial fuel cells, ISME J. 2 (2008) 519–527, https://doi.org/10.1038/ismej.2008.1.
[42] J. Tournebize, C. Chaumont, C. Fesneau, A. Guenne, B. Vincent, J. Garnier, Ü. Mander, Long-term nitrate removal in a buffering pond-reservoir system receiving water from an agricultural drained catchment, Ecol. Eng. 80 (2015) 32–45, https://doi.org/10.1016/j.ecoleng.2014.11.051.
[43] H.-Y. Cheng, X.-D. Tian, C.-H. Li, S.-S. Wang, S.-G. Su, H.-C. Wang, B. Zhang, H.M. A. Sharif, A.-J. Wang, Microbial photoelectrotrophic denitrification as a sustainable and efficient way for reducing nitrate to nitrogen, Environ. Sci. Technol. 51 (2017) 12948–12955, https://doi.org/10.1021/acs.est.7b0255710.1021/acs.est.7b02557.s001.
[44] K.P. Gregoire, S.M. Glaven, J. Hervey, B. Lin, L.M. Tender, Enrichment of a high-current density denitrifying microbial biocathode, J. Electrochem. Soc. 161 (2014) H3049–H3057, https://doi.org/10.1149/2.0101413jes.
[45] N. Pous, C. Koch, J. Colprim, S. Puig, F. Harnisch, Extracellular electron transfer of biocathodes : Revealing the potentials for nitrate and nitrite reduction of denitrifying microbiomes dominated by Thiobacillus sp, Electrochem. Commun. 49 (2014) 93–97, https://doi.org/10.1016/j.elecom.2014.10.011.
[46] Y. Yi, T. Zhao, B. Xie, Y. Zang, H. Liu, Dual detection of biochemical oxygen demand and nitrate in water based on bidirectional Shewanella loihica electron transfer, Bioresour. Technol. 309 (2020) 123402, https://doi.org/10.1016/j.biortech.2020.123402.
[47] P.A.G. Hofman, S.A. De Jong, E.J. Wagenvoort, A.J.J. Sandee, Apparent sediment diffusion coefficients for oxygen and oxygen consumption rates measured with microelectrodes and bell jars : applications to oxygen budgets in estuarine intertidal sediments, Mar. Ecol. Prog. Ser. 69 (1991) 261–272.
[48] L.P. Nielsen, N. Risgaard-Petersen, H. Fossing, P.B. Christensen, M. Sayama, Electric currents couple spatially separated biogeochemical processes in marine sediment, Nature 463 (7284) (2010) 1071–1074, https://doi.org/10.1038/nature08790.
[49] J.S.P. Ibánhez, C. Leote, C. Rocha, Porewater nitrate profiles in sandy sediments hosting submarine groundwater discharge described by an advection – dispersion-reaction model, Biogeochemistry 103 (2011) 159–180, https://doi.org/10.1007/s10533-010-9454-1.
[50] H.H.P. Fang, M. Zhang, T. Zhang, J. Chen, Predictions of nitrate diffusion in sediment using horizontal attenuated total reflection (HATR) by Fourier transform infrared (FTIR) spectrometry, Water Res. 42 (2008) 903–908, https://doi.org/10.1016/j.watres.2007.08.038.